

Fast Recovery of Robot Behaviors

George Council, *Member, IEEE*, and Shai Revzen, *Member, IEEE*

Abstract—If robots are ever to achieve autonomous motion comparable to that exhibited by animals, they must acquire the ability to quickly recover motor behaviors when damage, malfunction, or environmental conditions compromise their ability to move effectively. We present an approach which allowed our robots and simulated robots to recover high-degree of freedom motor behaviors within a few dozen attempts. Our approach employs a “*behavior specification*” expressing the desired behaviors in terms as rank ordered differential constraints. We show how factoring these constraints through an “*encoding templates*” produces a recipe for generalizing a previously optimized behavior to new circumstances in a form amenable to rapid learning. We further illustrate that adequate constraints are generically easy to determine in data-driven contexts. As illustration, we demonstrate our recovery approach on a physical 7 DOF hexapod robot, as well as a simulation of a 6 DOF 2D kinematic mechanism. In both cases we recovered a behavior functionally indistinguishable from the previously optimized motion.

Index Terms—robotics, recovery, constraints, templates, damage

I. INTRODUCTION

To associate the notion of “*autonomy*” with a putative “*agent*” implies that this agent has the ability to persist in carrying out its goals despite interference. The more profound the changes in action it manifests to continue achieving its goal, the more autonomous we perceive that agent to be.

Most modern robots achieve autonomous motion by implementing a sense-plan-act loop in which they rely on accurate models for predicting the consequences of potential actions. When robots are damaged or the environment undergoes a large change, the accuracy of the predictions falters, and full replanning in real-time becomes impossible because the models used for prediction cannot be reconstituted quickly enough.

Unlike robots, many animals display great aptitude at preserving motion despite changes in the underlying dynamics. Through injury, age, or the otherwise mutable nature of organic tissue, animals are able to preserve behaviors despite great dynamic variability. For example, in the case of light or moderate limb damage, we distinguish this resiliency from healing – a human with a sprained ankle immediately begins limping, rather than waiting for a healing process to restore the joint to full functionality. Obviously, robots would be advantaged by a similar ability to preserve task execution through damage or changes in dynamics.

Control theorists usually describe systems in terms of a differential generator – the “*uncontrolled dynamics*” – and the space of possible control actions at each state – the “*control distribution*”. The key insight behind our approach is the power of using the dual to the conventional control theory approach. We specify behaviors in terms of a (potentially over-determined) ranked list of differential constraints.

Many types of mechanical failure correspond to the removal or addition of kinematic constraints: e.g. a wheel loses traction removing a constraint, or a bearing locks adding a new constraint. We will show how in such cases our ranked list of constraints can be used to naturally define a reinforcement learning problem with a richly informative local gradient. The learning problem, enhanced by inclusion of additional “*natural*” constraints, converges much more rapidly than methods that lack this rich local information.

In our representation, high-ranking differential constraints represent unbreakable physical constraints imposed by physics and mechanical structure, whereas the lower-ranking constraints represent design choices and priorities. Whether constraints appear, disappear, or change, we always employ the dominant list of constraints to choose the robot’s action, thereby utilizing as much state-local information as possible. This mathematical representation makes it particularly easy to specify a desired behaviors using the conceptual framework of “*Templates and Anchors*” [1], [2, Chp.3].

This framework claims that in biology the movements of high degree of freedom “*anchor*” models that closely reflect the structure of the animal body in fact follow motions of a lower dimensional “*template*” model in which anchor degrees of freedom are coupled together tightly. We employed this insight by first selecting a lower dimensional collection of outputs which can reliably describe the desired outcomes, which we named the “*encoding template*”. We then specified the behavior in terms of differential constraints on the encoding template, and pulled those constraints back to the anchor system, thereby defining a non-holonomic system on what is typically the physical configuration space of the robot. Any anchor trajectories which satisfy these constraints map to the desired template behavior. For example, “walk straight across a room” could be expressed in terms of projection of the center-of-mass (CoM) on the horizontal, followed by constraining the CoM motion to be on a family of parallel lines, and also to have chosen a non-zero CoM velocity in the desired direction. Such a constraint on the projection is not a complete definition for a gait of a non-trivial legged robot, but any motion that met the lifted differential constraints would accomplish the objective of moving across the room.

The power of our dual constraint-based representation comes into play in that adding these designed constraints to the existing immutable physical constraints of the robot consists

Manuscript submitted May 1, 2020. This work was supported by ARO grants W911NF-14-1-0573, W911NF-17-1-0243, and W911NF-17-1-0306

G. Council is with the Department of Mechanical Engineering, Carnegie Mellon University, Pittsburgh, PA, 15213 USA (e-mail: gcouncil@andrew.cmu.edu)

S. Revzen is with the Department of Electrical Engineering, University of Michigan, Ann Arbor, MI, 48109 USA (e-mail: shrevzen@umich.edu)

©2020 IEEE. Personal use of this material is permitted. Permission from IEEE must be obtained for all other uses, in any current or future media, including reprinting/republishing this material for advertising or promotional purposes, creating new collective works, for resale or redistribution to servers or lists, or reuse of any copyrighted component of this work in other works.

of merely concatenating the designed constraints on the end of the list of physical constraints. Furthermore, when an ensemble of desirable anchor trajectories is available for training, a collection of data-driven encoding template constraints can easily be learned, added as low priority constraints, and used to assist the recovery of similar behaviors when needed.

There have been numerous authors that have considered the control of constrained dynamical systems with such geometric methods. Principal fiber bundles [3], Kinematic reduction [4], spanning killing forms [5], and other techniques from Riemannian geometry [6]–[8] (and the references therein), to name a few, are all powerful and general approaches to non-holonomic motion planning. Our approach uses less structure, and while our mathematical results are correspondingly weaker, we have an advantage in practice – the ability to learn constraints which produce a specific desirable trajectory, using a nearly arbitrary choice of outputs taking values in the encoding template. Thus our approach requires little to no model information to recover template trajectories, whereas the previous techniques typically rely on the availability of a precise model. In the work presented here we further differentiate ourselves from other constraint-based work in that we only attempt to recover a training example, although we could in principle extend to more general classes of training data.

Previous work has delved into the much more challenging problem of planning on a template, which requires that all template trajectories must always be liftable to the anchor. Because we only required that a single chosen trajectory be lifted, this greatly reduced the amount of structure we needed to impose on the problem. Below we demonstrate that our gait recovery technique is computable using data-driven methods applied to physical robots, and works rapidly in practice.

A. Mathematical preliminaries

We assume that a robot’s motion is determined by curves $x(t)$ taking values in a manifold Q_R on which we can write differential constraints. Typical choices for Q_R could be the configuration space of the robot body, its phase space [9], or a more general state space. While it may seem initially strange to allow the domain to vary so generally, we observe that a tangent vector [10], which is our fundamental object of interest, is naturally defined in an equally general setting.

We define a “*behavior specification*” to be a list of constraints of the form $\Omega_i(x) \cdot \dot{x} = \gamma_i(t, x)$, $i = 1, \dots, k$. Here each Ω_i is a differential 1-form [10] i.e. a section of the cotangent bundle T^*Q_R . The vector $\gamma(t, x) := (\gamma_1, \dots, \gamma_k)$ is a vector of length k that defines the value the constraint functions Ω_i must satisfy, and therefore takes values in the same codomain as that of the 1-forms. The list of Ω_i contains any inviolate physical constraints that determine the physics of the robot, as well as constraints we as designers wish to engineer into the system. Conventionally, the constraints could be written as a matrix: $\Omega(x) \cdot \dot{x} = \gamma(t, x)$, where the rows of Ω are the $\Omega_i(x)$. We assume the matrix Ω to be of constant, though necessarily not full, rank when evaluated along admissible curves of Q_R . Formally speaking, the behavioral specification is the pair (Ω, γ) .

A curve $x(t)$ taking values in Q_R which satisfies the behavior specification equation is an instance of the behavior. A major feature of our behavior representation is that it is agnostic of the mechanism that generates curves $x(t)$. In particular, instances of the behavior may intersect and even overlap, only to diverge later – unlike trajectories of conventional closed loop control models. With respect to a behavior specification there are only curves that satisfy the constraints, and those that do not.

We chose this definition for a behavior as it contains a number of special cases. For example, if Ω is invertible everywhere, we may write $\dot{x} = \Omega^{-1}(x)\gamma(t, x)$ – a conventional non-autonomous ordinary differential equation (ODE). Here instances of the behavior are solutions of the ODE. The popularly used class of affine control systems $\dot{x} = f(x) + G(x)u$ can be represented using a pseudoinverse G^\dagger of G , by constructing $\Omega(x) := I - G(x)G^\dagger(x)$ and $\gamma(t, x) := \Omega(x)f(x)$. This is a standard application of control redesign. If the space Q_R is taken as the configuration space of a mechanical system, Pfaffian and affine differential constraints are behavior specifications as well. In kinematic reduction, the constraints would be the metric inner products of [4]. The preceding list of model types that can be realized as behavior specifications is not exhaustive, but is intended to indicate that a number of useful constructions of control and robotics are naturally encapsulated in our proposed definition.

While the constraints required by physics are intrinsic to the system, it is not immediately clear from the definition given how to encode a design goal into a collection of constraints. We propose the following strategy: we first find a manifold Q_E and a full-rank function $\phi : Q_R \rightarrow Q_E$ such that we are certain that whatever outcome we desire is realized by a behavior specification on Q_E . We call the space Q_E an “*encoding template*”, as it encodes all the necessary information. Generally, we take the dimension of Q_E to be less than that of Q_R . The map ϕ reduces the coordinates of Q_R to values we as designers care about encoding; for example, ϕ could return the CoM coordinates, an end effector location, joints angles, etc. The map ϕ can equally be considered a collection of “*outputs*” $y_i := \phi_i(x)$. We write the behavior specification $\omega_i(y) \cdot \dot{y} = \eta_i(t, y)$ on the output variables / encoding template. Such a construction precisely includes all the special cases a behavioral specification can capture, but only on the output variables. We can then pull the ω_i back to Q_R to augment any extant Ω by Ω_j . In matrix form, pulling back is merely adding rows $\Omega_j(x) := \omega_j(\phi(x)) \cdot D\phi(x)$ to the matrix Ω . We augment our notation to include ϕ in the behavior specification as the tuple (ϕ, ω, η) , indicating that it is the image of ϕ which is the target of our design efforts, emphasizing that there are virtual constraints on the output variables in concert with pre-existing constraints that are defined only on Q_R .

B. Recovery via constraints

From here on we restrict our interest to the recovery of a behavior on a robot post-disruption. We assume that there was a distinguished curve $x_0(t) \subset Q_R$ that satisfied a

given behavior specification (ϕ, ω, η) . For emphasis, we will consider the case where the number of constraints *exceeds* the dimension of Q_R , but that the virtual constraints ω are satisfied without control effort. In this case, the rows defined by ω are redundant with the rows of Ω – the rank of ω augmenting Ω is identical to that of Ω alone along desired trajectories in Q_R . Thus, at this point we have three classes of constraints: Ω_P that come from the underlying physics, Ω_D which are design constraints derived from the (ϕ, ω, η) specification, and Ω_L constraints that were learned from the encoding of the example $x_0(t)$, i.e. by observing $\phi(x_0(t))$. These constraints can be viewed as if they are enforced in an order of priority $\Omega_P \gg \Omega_D \gg \Omega_L$; here we indicate priority by \gg .

We assume that the robot is disrupted in a manner that introduces a new Ω_r to Ω_P , or eliminates one of the native Ω_i that comprise Ω_P , representing effects such as motors seizing, limbs breaking off, etc. The recovery strategy is to re-enforce, via control, the design constraints Ω_D , which are presumably violated by whatever motion the broken robot is performing without compensation. If the rank of Ω_P was reduced, the learned constraints Ω_L which were originally redundant, can play an essential role in completing the behavior specification to full rank.

We have assumed $\dim Q_E < \dim Q_R$, and that the behavior specification (ϕ, ω, η) is satisfied by the example trajectory x_0 , which was presumably obtained from a computationally intensive offline optimization. Thus we know:

$$\forall j, t: \omega_j(\phi(x_0(t))) \cdot D\phi(x_0(t)) \cdot \dot{x}_0(t) = \eta_j(t, \phi(x_0(t))) \quad (1)$$

From the constant rank assumption about $\phi(\cdot)$ we obtain that for each $x_0(t)$ there is an entire manifold of possible values for a new instantiation $x(t)$ such that $\phi(x(t)) = \phi(x_0(t))$.

Before damage, we took (Ω, γ) as $(\Omega_P, \gamma_P) \gg (\Omega_D, \gamma_D) \gg (\Omega_L, \gamma_L)$ and used the first $\dim Q_R$ linearly independent constraints of these determine the velocity $\dot{x}(t)$. However, by virtue of the addition of Ω_L , the total number of constraints in (Ω, γ) is larger than $\dim Q_R$ (i.e. Ω is tall), and these constraints are redundant on the instantiation of the behavior $x_0(\cdot)$. As long as the robot was functioning without damage, the $\Omega_D(x_0) \cdot \dot{x}_0 = \gamma_D(t, x_0)$ constraints were satisfied by assumption, and no change in control was needed.

Damage to the robot was a low rank change to Ω_P , replacing it with $\tilde{\Omega}_P$ instead, of possibly lower or higher rank, but such that only a few constraints are affected. In other words, only a few rows of Ω_P and γ_P are changed due to damage. Consider the case where the rank change, i.e. change in number of constraints, associated with this damage to Ω_P is such that

$$\dim Q_R - \text{rank } \Omega_L \leq \text{rank } \tilde{\Omega}_P + \text{rank } \Omega_D \leq \dim Q_R \quad (2)$$

When (2) holds, the change in rank induced by the damage can be taken up by removal or addition of learned constraints Ω_L , and we could solve for new feasible velocities without harming compliance with any of the design constraints $\Omega_D(x) \cdot \dot{x} = \gamma_D(t, x)$.

Here the use of the dual representation in our behavior specification came into its own. It allowed us to gracefully recover from structural changes in the constraints governing the robot. If an explicit form of $\tilde{\Omega}_P$ is known, finding a

recovery trajectory requires no optimization to be done – it follows directly from integrating the new behavior specification equation with the modified constraints; we demonstrated this in §II-A below.

In the case of a physical robot, the modified constraints might not be known; we explored this possibility by attempting to re-learn a walking behavior for a hexapedal robot. For this, optimization is a natural tool. Taking a motion over time $t \in [0, T]$, using control input $u(t)$, and producing trajectory $x(t)$, it is common to express cost as an integral. For a behavior specification, this suggests a natural choice of cost function:

$$J[x, u] := R[u] + \lambda \int_0^T \|\Omega_{D,L}(x) \cdot \dot{x} - \gamma_{D,L}(t, x)\|^2 dt \quad (3)$$

The function R penalizes the input, while the remainder penalizes the failure to meet the behavior specification (in the Ω_D, γ_D part) and penalizes any other discrepancies from the encoding of the example (in the Ω_L, γ_L part). The constraints explicitly measure and penalize directions of \dot{x} which, by virtue of carrying through ϕ are deemed relevant.

We used this approach in our hardware-in-the-loop optimization in section II-B. In this task we were only concerned with the end-point of the robot motion and therefore we took the control cost functional $R = 0$. For a manually tuned gait which walked forward, we learned a behavior specification (Ω_L, γ_L) using a choice of encoding template motivated by the Lateral Leg Spring (LLS) [11] and Spring Loaded Inverted Pendulum (SLIP) [12] dynamic templates. We then initialized the optimization with a gait that left the robot stationary, and ran it with the violation of constraints norm and no end-point goal. This optimization allowed our robot to re-learn an effective forward gait in 36 iterations.

C. Relation to geometric mechanics

An important special case which motivated much of our work was the case where the output variables can be split into components $y = (s, g)$, with the s variables being the directly controllable robot “*shape variables*”, and the g variables being controlled through the intermediate action of s , \dot{s} , and the constraints. Typically, g represents global position and orientation of the robot or of an object the robot is manipulating.

The behavior specification constraints can be written as

$$\omega(s, g) \cdot (\dot{s}, \dot{g}) = \gamma(s, g) \quad (4)$$

When the space Q_E is a configuration space and $\gamma(s, g) = 0$, equation (4) coincides with the familiar Pfaffian-constraint case.

The application of the forms $\omega(s, g)$ to (\dot{s}, \dot{g}) can, from linearity, always be re-written as $\omega_s(s, g) \cdot \dot{s} + \omega_g(s, g) \cdot \dot{g}$, where ω_s and ω_g are left and right blocks of the matrix form of ω with $\dim s$ and $\dim g$ columns respectively.

If ω_g has a left inverse ω_g^\dagger , we can obtain for any given $s(t)$:

$$\dot{g} = \omega_g^\dagger(g, s) (\gamma(t, g, s) - \omega_s(g, s) \cdot \dot{s}), \quad (5)$$

a non-autonomous differential equation for g . Thus, enforcing the constraints of equation (4) uniquely determines the curve

$g(t)$ from $s(t)$ and the initial $g(0)$. In other words, if we maintain the related (Ω_D, γ_D) , it ensures that the robot moves the same way through space, or manipulates the object it is moving in the same way. The typical case where such a “reconstruction equation” appears is in the “non-holonomic connection” of [3], [13]–[16], and the references therein.

II. RESULTS

A. Crawler

As our first example, we present a simulated two-armed robot pulling itself on a plane. The robot is depicted in Fig. 1. Each arm is a linkage that consists of four rigid bars connected end-to-end by powered swivel joints. Our objective was to preserve the motion of the body when one of the joint actuators is jammed. We implemented this example in Python 2.7.5 with the `numpy` and `scipy` numerical processing libraries. The complete source code can be obtained as a git archive available at <http://birds.eecs.umich.edu/crawler-recovery.git>.

We took the configuration space Q_R of the robot to be $(x, y, \theta_0, \theta_1, \dots, \theta_6) \in \text{SE}(2) \times \mathbb{T}^6 = G \times S$. This comprises the center-of-mass position (x, y) and orientation θ_0 within the plane, which we collectively denote with $g := (x, y, \theta_0)$, and the six joint angles $\theta_j, j = 1 \dots 6$, which we collectively refer to with $\theta_V := (\theta_1, \dots, \theta_6)$. The latter are intrinsic, i.e. relative to the body and symmetric under translation and rotation of the center-of-mass; they are thus shape variables.

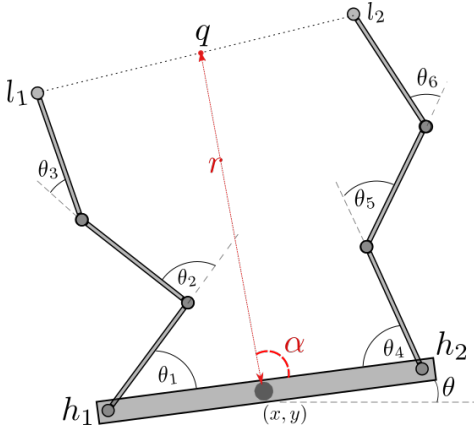


Fig. 1: Illustration of our crawler. The grey members indicate components that belong to the robot. The points l_1 and l_2 are fixed foot locations. Each joint θ_j is a powered rotational joint. The points h_1 and h_2 are the attachment points at which the limbs attach to the body. The center point of the foot locations q defines the value r and angle α (in red), which are our choice of encoding template.

Our robot moved by attaching to the plane at the two locations l_1 and l_2 with freely rotating pivots, dragging itself with its limbs. Let us consider the problem of preserving this body motion when the two leg attachment points l_1 and l_2 are fixed, but a joint motor jams.

The robot is a kinematic system, so that the positions l_1 and l_2 and angles θ_j jointly define holonomic constraints which are the native physical constraints Ω_P on Q_R . Using complex

numbers to represent the plane, the following equations compute the endpoints of the limbs f_1 and f_2 as a function of $(x, y, \theta, \theta_1, \dots, \theta_6)$:

$$f_1 := x + iy + e^{i\theta} (h_1 + e^{i\theta_1} (1 + e^{i\theta_2} (1 + e^{i\theta_3}))) \quad (6)$$

$$f_2 := x + iy + e^{i\theta} (h_2 + e^{i\theta_4} (1 + e^{i\theta_5} (1 + e^{i\theta_6}))) \quad (7)$$

The robot is subject to the (holonomic) constraints $\frac{d}{dt} f_1 = 0$ and $\frac{d}{dt} f_2 = 0$. These are four constraints on Q_R that make up Ω_P , with $\gamma_P = 0$ (we treat the real and complex components as separate equations).

We arbitrarily chose the parameters l_1, l_2, h_1 , and h_2 to be as shown in Table. I. These choices roughly match the proportions in Fig. 1.

TABLE I: Crawler Parameters

Parameter	Value
l_1	$+2.5 + i2$
l_2	$-2.5 + i2$
h_1	$+1$
h_2	-1

Our desired motion is depicted in Fig. 4. The traces labeled “desired” are the nominal inputs without damage. This roughly corresponds to a serpentine pattern from the CoM, and it is this $g(t), t \in [0, 1]$ we wish to maintain. The required inputs $\theta_j(t)$, which we jointly refer to as θ_{orig} , are shown in radians in Fig. 2. In the notation of section I-A, $(g(t), \theta_{orig}(t))$ is the nominal $x_0(t) \in Q_R$.

We now define a choice of encoding template Q_E . Let the point $q \in \mathbb{C}$ be the midpoint of the two foot locations l_1 and l_2 . We define the encoding template $Q_E = \text{SE}(2) \times \mathbb{R} \times S^1$ as the body frame, with additional $(r, \alpha) \in \mathbb{R} \times S^1$, as shown in red in Fig. 1. The template shape coordinates are the distance r of the CoM to the point q , while α is the angle of the robot body with w.r.t line $q - (x, y)$ which we encode via (8).

$$r \exp(i(\theta_0 + \alpha)) + x + iy = q \quad (8)$$

This definition of encoding template defines a map $(x, y, \theta, r, \alpha) = \phi(\theta_1, \dots, \theta_6)$, which expresses the notion that while we cared about the $\text{SE}(2)$ location of the body of the robot, and the relative location of the robot to q , we did not care about specific actuator angles except inasmuch as they influenced those outputs. Solving (8) for r and α in terms of the θ_i, h_1, h_2, l_1 , and l_2 , we obtain ϕ . Again, we point out that there are two independent equations determined by (8), as we solve the real and imaginary parts separately. Note that this implies ϕ is the identity map on the (x, y, θ) coordinates representing the robot body in $\text{SE}(2)$. We evaluated ϕ along our original trajectory, yielding the desired output $y(t)$ in the encoding template. We denoted the resultant shape component of $y(t)$ by $(r_0(t), \alpha_0(t)) \in \mathbb{R} \times S^1$ (see Fig. 2).

For the encoding procedure to fully define a desirable motion, we needed there to be a unique velocity $(\dot{x}, \dot{y}, \dot{\theta})$ determined by each pair $(\dot{r}, \dot{\alpha})$. By directly differentiating (8), we obtained two Pfaffian constraints ω_1 and ω_2 , that relate $(\dot{r}, \dot{\alpha})$ to \dot{g} , with $\gamma_D^1 = \gamma_D^2 = 0$. Additionally, our choice of ϕ defined two equations, which when differentiated, yielded

the template constraints $\omega_3 := \mathbf{d}\alpha$, $\gamma_D^3 := \frac{d}{dt}\alpha_0(t)$, $\omega_4 := \mathbf{d}r$, and $\gamma_D^4 := \frac{d}{dt}r_0(t)$. To match the dimension of G , a final independent equation was necessary.

As our designed behavior specification, we chose the constraint

$$\omega_5 := \mathbf{d}x - \mathbf{d}\theta; \quad \gamma_D^5 := 0 \quad (9)$$

Since this constraint is only on group variables, which are unchanged by ϕ , this constraint is unchanged when pulled back to Q_R as $\Omega_D^5 := \mathbf{d}x - \mathbf{d}\theta$. This virtual constraint augments the holonomic constraints of ω_i to generate three equations that define Ω_D so that (5) is solvable. This last, arbitrarily chosen Ω_5 , is a design choice – i.e. in Ω_D . We could have equally used an example motion and a learned constraint Ω_L .

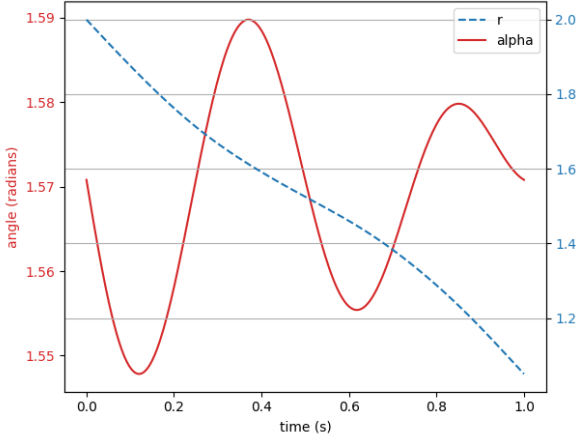


Fig. 2: r and α coordinates of the template along the θ_{orig} curve, i.e. the desired reference trajectory on the template.

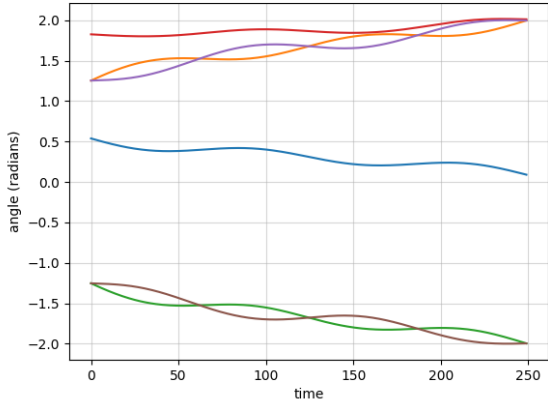


Fig. 3: The six joint angles of θ_{orig} corresponding to $x_0(t)$

We now assumed that the θ_1 actuator is jammed. We expressed this by adding a differential constraint $\mathbf{d}\theta_1$ to Ω_P whose value is identically 0. The addition of this constraint modifies Ω_P to $\tilde{\Omega}_P$, which is one row longer. If we did nothing, and simply played back the un-jammed components of θ_{orig} with the θ_1 actuator stuck, we would obtain considerable error in the encoded $(r, \alpha, x, y, \theta)$ motion. In Fig. 4

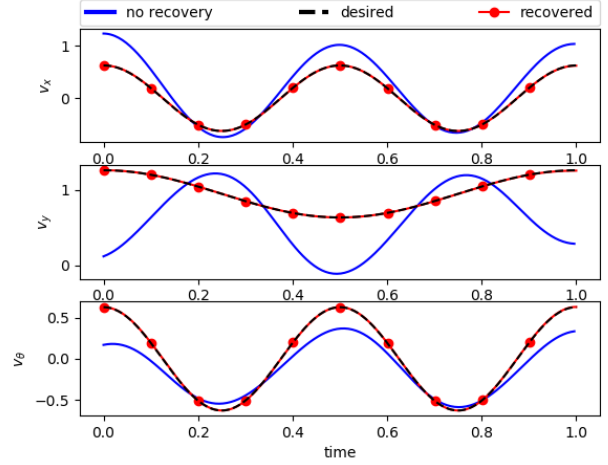


Fig. 4: The COM group velocity $\dot{g} = (v_x, v_y, v_\theta)$ over time. The “desired” curve (black dashed) is the undamaged motion that we are aiming to recover. The “old” curve (blue solid) is the group velocity achieved if no recover strategy is attempted post damage. The “recovered” trace (dots; red solid) is the performance after recovery.

the curve labeled “old” illustrates the resulting velocity of the CoM should “playback” be attempted without some form of recovery.

We thus employ the constraints ω_i we determined above. Pulling these constraints back to Q_R defines Ω_D , and combining them with Ω_P we obtain a six-dimensional non-autonomous differential equation that can be integrated to generate a desired motion (for more details, see [17]). While a six dimensional system may initially seem contradictory, the jamming constraint is very clearly integrable, the six dimensional equation is evolving on a five-dimensional submanifold, which gives us the required $\theta_2, \dots, \theta_6$ we desire.

The solution of this equation is the θ_V that generates the same desired COM motion despite the seized limb, if such a solution exists. Numerically integrating, we obtained a new $\theta_V^{rec}(t)$, $r(t)$, and $\alpha(t)$, shown in Figs. 2 and 5. Note that we cite Fig. 2 for the new encoding template curve as well; this is intentional, as the new and old encoding template curves are numerically identical.

The performance of our recovered joint inputs is shown in Fig. 4 as the “recovered” trace. It appears to recover the desired CoM velocity (and thus, group position) to within visible accuracy. This is especially notable in contrast to no recovery at all (the “old” trace in Fig. 4).

B. Hexapod robot

To test this approach on a physical device, we needed an appropriate encoding template. For biomechanists, the difference between “running” and “walking” is defined in terms of the energy reservoirs participating in the exchange generating the motion. In walking, potential energy exchanges with kinetic energy by vaulting over a rigid leg; thus ground speed is lowest when the center-of-mass is highest. In running,

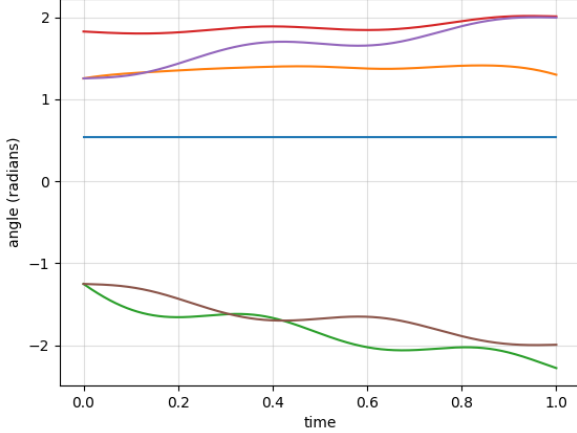


Fig. 5: The recovered joint angles $\theta_V^{rec}(t)$. As expected, with a jammed joint, one angle is constant. The other limb angles have been adjusted to compensate for the jamming constraint.

elastic energy of stretched tendons and muscles exchanges with kinetic energy; thus ground speed is highest when the center-of-mass is highest. Thus, the kind of gait appearing (running vs. walking) can be encoded in terms of total energy in these reservoirs. We designed a six-legged robot to facilitate the measurement of elastic energy storage in its legs. This, we hoped, would allow us to define an encoding template in terms of these energy exchanges, and test our strategy on a physical device.

The robot (“Enepod”) is depicted in Fig. 7. It consisted of a chain of 7 motor modules (Robotis Dynamixel EX106 and MX64) as an actuated backbone, connected to six passive spring steel (1/16” #1075) legs. The legs were mounted to the EX modules, as they provide more torque. The springs were flexible enough to exhibit deflections of more than 1 cm at the foot during motion making it feasible to sense their deflections using a motion tracking system. This provided an instantaneous window into the elastic energy stored in the body at any given time.

We generated a robot gait as a sequence of timed position commands which were carried out by individual control loops in the motor modules. The gait we chose was an “*alternating tripod*” gait analogous to that used in the RHex hexapod [18]. In this gait the feet are grouped into two collections of three feet (“*tripod*”). Feet in a tripod moved in phase with each other, and anti-phase with the feet of the other tripod. If the system were perfectly rigid, each tripod would be undergoing an identical motion. With elastic legs, even though they receive the same commands, the dynamics of the body and of contacts alter the response. Such flexible limbs would have been a major challenge for a dynamic model. However, since our method does not need a predictive model we did not encounter this difficulty.

As is appropriate for a periodic gait, we analyzed the motion of the robot with respect to a kinematic phase estimate [2] obtained using the tool *Phaser* [19] from motion tracking data collected with a retroreflective tracking system (Qualisys; with

10 Opus-310 cameras at 250 FPS; Qualisys Track Manager v2.17 software interfaced to custom python SciPy 1.0.0 code using the Realtime API v1.2.

The space of gaits we considered is spanned by the parameter space $\mu \in [-1, 1]^5$. The values of μ determined the signal that drives the center module MC (see Fig. ??). The other six modules input signal remained unchanged. We compared convergence rates for optimizing μ with respect to a conventional cost function to optimizing μ with respect to a learned behavior specification Ω_L .

We performed this process in two stages. In the first stage, we manually designed a gait that achieved forward translation. Using the notation used in §I-A, this nominal gait is $x_0(t)$. We then evaluated our chosen output functions – chosen for being obvious stand-ins for energy reservoirs – along this cycle. We constructed a representation of the functions’ values as a Fourier series in phase. Using this model, we differentiated to obtain the necessary ω_i , and η_i . By pulling back these functions to the original state-space using our numerical estimate of phase, we obtain $(\phi, \Omega_L, \gamma_L)$ — the “*learned constraints*” that we introduced in §I-B. We used these Ω_L to define a cost function J , exactly as in (3).

1) *Encoding Template*: We defined four output functions whose images, together with phase, comprise the encoding template. These outputs were the vertical and horizontal deflections of each of the two tripods. The intuition behind this choice of outputs was that: (1) the tripods act independently; (2) the legs in a tripod can trade off each other; (3) the vertical and horizontal bending of the legs was, by design, independently taken up by different springs; (4) vertical and horizontal bending is expected to occur at different phases. Thus each tripod had two elastic energy reservoirs, one each for horizontal and vertical deflections, expected to act at different phases. This can easily be seen from the horizontal and vertical projections of the classical Spring Loaded Inverted Pendulum model [12]. The phase dependent changes in these tripod-average deflections constituted the learned constraints Ω_L that we employed in lieu of any other model information to characterize our desired motion and produce a behavior specification violation cost, exactly as described in (3).

We calculated the vertical spring deflection $V_i, i = 1, 2$ from marker locations, coding it as an angle rather than as a linear displacement. This angle, between the horizontally orientated spring-steel members and the central spine, is monotonically related elastic energy stored (according to e.g. beam theory), was easy to measure given our instrumentation, and we found it empirically to vary in a periodic manner. We collected six distinct vertical deflection angles at every time-step despite the left and right angles resulting from the deflection of the same double-sided leg, because each leg was clamped to the body in its middle, allowing each side of a leg to bend independently in the vertical direction. Fig 9 depicts an example time series collected from the Enepod striding forward with its limbs cycling at 2 Hz.

We measured the fore-aft deflection of the vertically-mounted springs (e.g. the deflection in the horizontal direction) differently from the vertical deflection. We used the marker sets indicated in Fig. 7 to define the two centroids - C_{top}^i , and

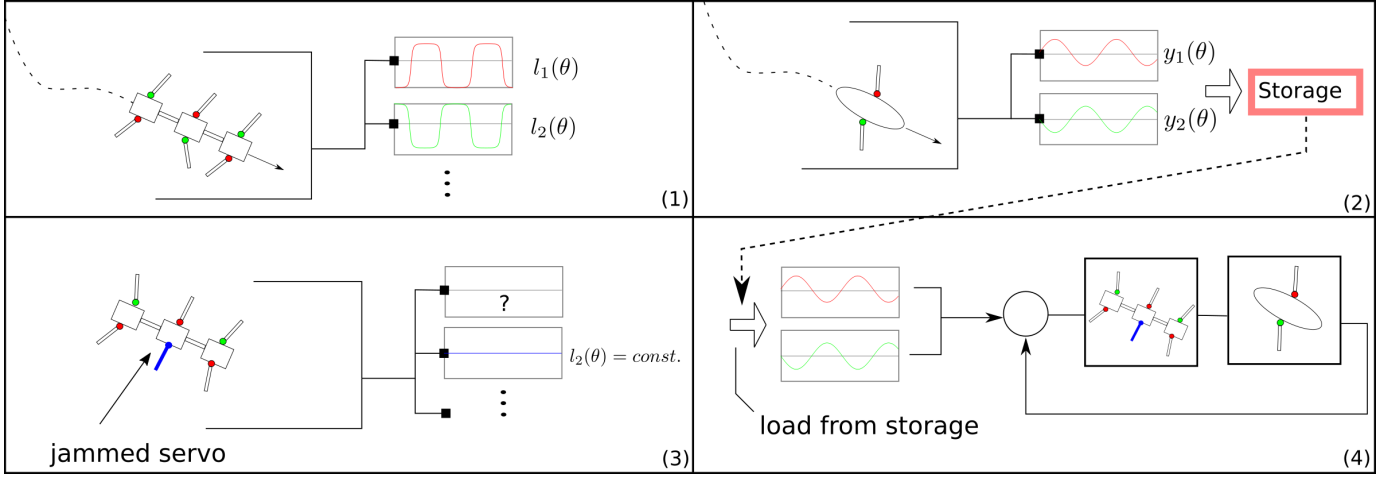


Fig. 6: Overview of the fast recovery process. **(Training)** Assume an existing desired behavior $x_0(t)$ is found for the robot (here a hexapod; (1)) using control $u(t)$, e.g. via costly optimization. It satisfies both physical Ω_P and design Ω_D constraints: $\Omega_{P,D} \cdot \dot{x}_0 = \gamma_{P,D}$. Project its state down to a candidate encoding template by identifying a collection of observations sufficient for representing the desired behavior (here a sprawled biped; (2)), thereby selecting ϕ . Selecting further a collection of learned constraint forms ω on this template. Learn and record the $\eta(t) := \omega(\phi(x_0))D\phi\dot{x}_0$ of (1) in memory, and store the pullback of ω , the learned constraints $\Omega_L := \omega \circ \phi \cdot D\phi$. **(Recovery)** Robot has failed (blue leg has jammed motor in (3)); it has a new physical Ω_P^* . If the new Ω_P^* is known, pick a subset Ω_L^* of Ω_L such that together $\Omega_P^*, \Omega_D, \Omega_L^*$ are exactly full rank, and solve for a new \dot{x} which will recover the behavior (e.g. in (4)). If Ω_P^* is not known, iteratively learn a new control u^* minimizing the constraint violation cost $J[x^*, u^*]$ of (3). This cost function admits x_0 as an optimum if it is achievable, and all its optima have the same encoding template motions as x_0 (e.g. in (4)). Since the cost function has a richer gradient, the optimization can converge much faster than the naive optimization that created x_0 in (1).

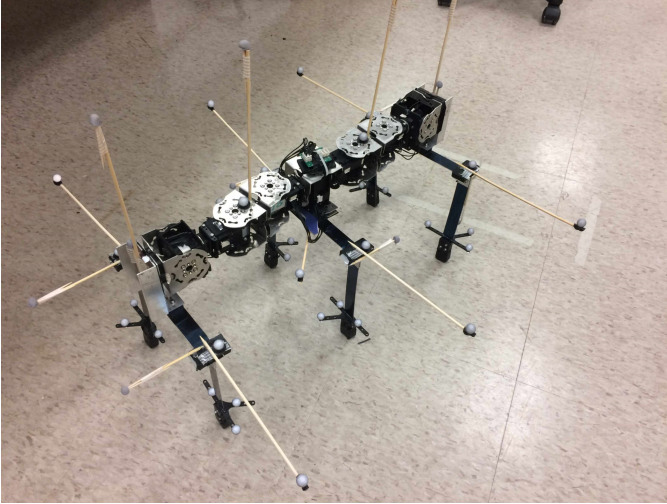


Fig. 7: The Enepod robot. We mounted retroreflective markers on wooden spokes, increasing our resolution for measuring deflections of the legs in real time using the marker motion tracking system.

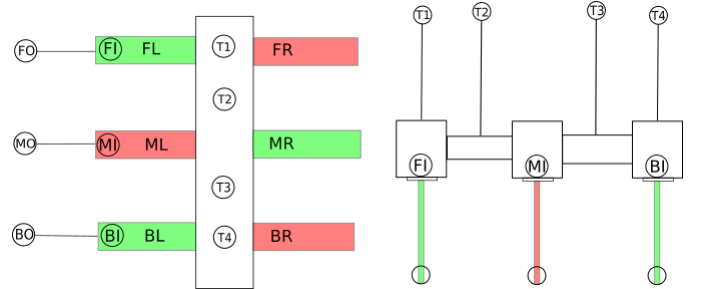


Fig. 8: Leg groupings on the Enepod. The grouping (BL,MR,FL; in green) defines the “left tripod” of legs, which move in phase which each other, and antiphase to the “right tripod” (BR,ML,FR; in red). This grouping of legs was used for both horizontal and vertical springs. Some markers have been omitted for visual clarity.

C_{foot}^i , respectively, where i indexes the leg. We projected these two centroids into the (x, y) plane, and performed a principal component analysis [20]. The first two principal component projections, taken as a function of phase are the two horizontal outputs H_1 and H_2 (see Fig. 10). Physically, there are two principal axes of horizontal deflection, representing two elastic energy reservoirs associated with horizontal bending, but it

turned out that these axes do not correspond to bending parallel to the major line of the central spine.

2) *Goal function*: We built a nominal value for each output function by measuring its value while the robot was executing the nominal gait ($x_0(t)$). By computing and caching Fourier-series approximations of the output functions, we defined the constraints. As can be seen in Fig. 10 and Fig. 9, these output functions are strongly periodic and lack apparent spectral complexity, allowing an order 4 Fourier series to fit them well within measurement noise. For the disrupted robot, we used these Fourier series to define the cost function as shown in (3).

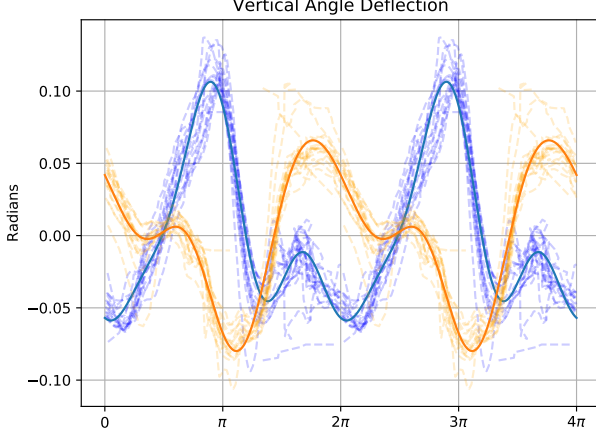


Fig. 9: Summed vertical deflection signals for tripod one and two, unwrapped over two periods. We plotted the value as function of phase in individual strides (dashed line), and the Fourier-series fit of order 3 to $n = 15$ strides (solid line)

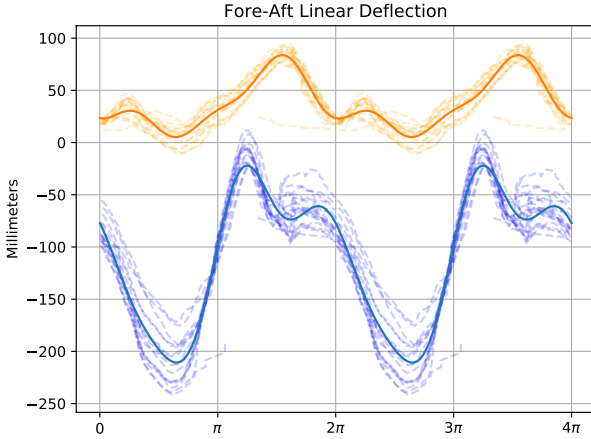


Fig. 10: Horizontal deflection outputs. These are the first two principal components of the fore-aft deflection data (H_1 and H_2) over two periods. We plotted their values as function of phase in individual strides (dashed lines), and the Fourier-series fit of order 3 to $n = 15$ strides (solid lines). This suggests that the two reservoirs are approximately 90° out of phase.

As the robot is not perfectly periodic, to evaluate the cost function for each choice of parameters, we used a windowed average of the goal functional over windows of $n = 35$ strides (cycles). We fixed the gait frequency at 2.5 Hz, giving a duration of $t_f = 35 \times \frac{1}{2.5} = 14$ sec for each cost function evaluation.

3) *Optimization results:* We conducted the optimization using the Nelder-Mead algorithm on the μ parameters that define the signal driving the central module.

The evolution of the cost is displayed in Fig. 12. We terminated the optimization after we had approximately reduced the

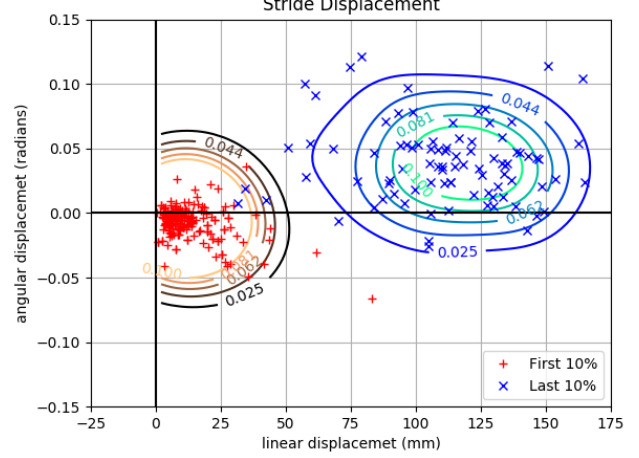


Fig. 11: A comparison of pre and post optimization. We represented $\xi = (\xi_x, \xi_y, \xi_\theta)$ by the 2D position with $x = (\xi_x^2 + \xi_y^2)^{1/2}$ and $y = \xi_\theta \in [0, 2\pi]$. We plotted the results of individual strides (first 10% of strides red “+”; last 10% blue “x”) and the contours of a kernel smoothed density produced from those data (black to orange contours for first 10%, blue to cyan for last 10%).

cost by 40%. Our choice for this was empirically motivated: the robot had achieved acceptable performance, as depicted in Fig. 11. This termination condition is fairly arbitrary, and future work will include a more principled approach for determining termination. After $n = 36$ iterations, where a single iteration corresponds to 35 ± 1 cycles executed at a set of hyper-parameters μ , the mean displacement per stride was significantly enhanced.

The distribution of motion outcomes at the end of optimization is wider (Fig. 11), but one should keep in mind that Nelder-Mead inspects some poor parameter choices in iteration 26 and 33.

The key result is that with $N = 36$ iterations, without a predictive model of the robot, and without directly measuring the robot’s motion in the plane — which is the actual goal for the original gait optimization — we were able to regenerate useful forward motion which is nearly as effective as the initial optimization. All this was done by enforcing constraints that were learned by measuring the working robot.

III. DISCUSSION

We have shown that by using our newly defined notion of a “behavior specification” and “encoding template” we can not only represent a broad class of existing physical dynamics and control problems, but also model an important class of failures — namely the loss or addition of constraints — as a deletion or insertion of rows in this specification. Given the problem of recovering a robot behavior after such a failure, we have shown solutions for two cases. When the post-failure specification is known, we demonstrated a closed form solution (see II-A). When the post-failure specification is not known, we have shown how a reasonable choice of virtual constraints learned

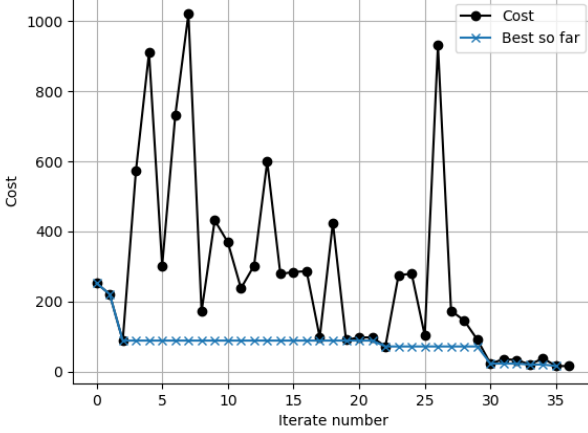


Fig. 12: Performance of the cost function by iterate. Plot shows the absolute cost at the i -th iterate (dots, black), and the best-cost-so-far (“x” marks, teal).

by observing the encoding template projection of the desired behavior can be used to rapidly (re-)learn an equivalently desirable behavior (see II-B).

The core property we exploit is a trivial feature of linear equations: if there are m equations in n variables, and $n > m$, there is a specific solution v_s , and a nullspace of values v_n such that $v_s + v_n$ is still a solution.

By keeping track of the linear/affine differential constraints which comprise the behavior specification, we preserve the ability to exploit the nullspace of velocities that preserve our behavior specification as the system changes. The addition or removal of constraints drops or activates low priority constraints, buffering our scheme against the violation of the design constraints Ω_D . If through control we can force a damaged system to move within the desired nullspace the resulting behavior will be identical, and any solution that exactly restores the desired behavior must be of this form. Even if we cannot force the constraint violation cost function (3) to zero, using it brings us closer to a desirable behavior while being neutral to changes that have no effect on the desired outcomes.

A. Specialization of the result to locomotion

Robots designed for locomotion often have a natural partition of their configuration space [13]: the body frame evolves in $SE(3)$ or a subgroup thereof, while other, more arbitrary dynamics account for the motions of the limbs (more generally, variables which determine the shape of the robot). This natural splitting of variables exists in all systems that are symmetric under a Lie group of transformations. Such a configuration space is locally of the form $Q = S \times G$ where S is the shape space and G is a group representing the symmetry of the environment, typically sub-group of $SE(3)$. The interaction between the body-frame, body, and world is mediated by constraints that differentially relate body-frame velocities to limb velocities. Usage of so-called “principal G connections”

in this context has demonstrated that the our required structure is present; indeed, if the constraints are symmetric under G , (5) is little more than a “non-holonomic connection” [3] expressed in coordinates. Our construction is effectively postulating that we can assign a connection to the template, and pull this connection back to the anchor.

It is often convenient to write models such that: (1) the space $Q_R = S_R \times G$, and that (2) the map $\varphi = (\varphi^S, \text{id}_G)$ is identity on the group G , and $\varphi^S : S_R \rightarrow S_E$, for $Q_E = S_E \times G$. This assumption corresponds to identifying an encoding template Q_E that has the same body-frame (usually taken to be the center-of-mass frame) as the full robot. For example, if we had a six-legged robot that moved in the plane, we could have an encoding template that was a kinematic car whose center-of-mass and body axes coincided with the robot’s for all time. Then, by recovering the chosen trajectory of the kinematic car, the group motion of the anchor robot is also preserved, even though the robot’s limb motions may be very different from their original behavior.

A helpful advantage of a system that is symmetric under a group G is that the dimension of G is a known constant. Thus, we could immediately obtain the number of required constraints necessary to determine a desired $g(t)$. If the group has dimension d , we necessarily and sufficiently require that we have d linearly independent constraints in the behavior specification. When this condition is satisfied, $g(t)$ is uniquely determined by a given $s(t)$.

B. On the choice of output functions

Unlike the classical approaches of mechanical modeling, we point out that the behavior specification constraints do not need to be direct descriptions of constraint forces attributed to the robot’s mechanical structure. The constraints can be written in terms of outputs evaluated on examples of the desired behaviors – differentiated, they define the Ω_L constraints that are required to be satisfied.

At the extreme, recall the behavior specification of a reference trajectory: the constraint forms are $\omega_i := dy^i$ and we can use the value constraints $\eta_i(t) := \frac{d}{dt}y_j(t)$. If $\dim Q_E$ such constraints were defined, this is merely a representation of a desired reference $y(t)$ to be tracked, given a fixed initial condition $y(0)$. However, these constraints need not be expressed in terms of the native coordinates y_i of Q_E . Another version of this same argument is when the ω_i are the derivatives of “output functions” $f_j : Q_E \rightarrow \mathbb{R}$. As long as the collection of derivatives ∇f_j is full rank, the chain rule allows constraints to be synthesized just as effectively in terms of the f_j – an arbitrary choice of output variables y – allowing those to be selected for convenience of measurement.

We both emphasise, and have demonstrated, that experimental data is completely adequate to build such constraints, as long as data is sufficiently rich to support a suitable collection of locally defined output functions. To define η , the robot can execute its desired motion, and the time-series that results from evaluating the output functions is η by definition. The recovery problem is to restore this time series via control. The usage of output functions in such a manner mitigates the need to

develop any predictive model, such as the dynamics of the robot, which is generally a challenging task.

The condition of sufficient rank is essential to our process, and likely translates in practice to a need for a sufficient rank and a good condition number. Since by assumption the dimension of Q_R is greater than that of Q_E , it can be shown with straightforward transversality arguments (e.g, Chapter 2 of [21]) that the set of output functions that are adequate to meet our necessary rank condition is an open and dense set (full details of this argument are given in [17]). Intuitively, its unlikely that randomly selected vectors are linearly dependent in a high-dimension space, and very rectangular random matrices will generally have good condition numbers.

More generally, the differential constraints themselves can be considered “*output functions*”, only that their domain of definition is TQ_E , rather than Q_E . For any differential form ω , it can always be evaluated on a given observed output curve to return a time sequence of values η . Thus, we need not be restricted to ω choices that arise as exterior derivatives, i.e. non-exact forms can also be used. A designer is free to employ real-valued functions of Q_E and use their exterior derivatives, or to directly define linear functions of velocity, i.e. differential forms, on TQ_E .

C. Behavior Specifications can represent kinematic synergies

In biomechanics the concept of “*kinematic synergies*” is used to represent the observation that animal muscle actuation is often coordinated in such a way that motions occupy low dimensional subspaces of the space of possible actuation combinations (e.g. human manipulation tasks [22]–[24]).

From a formal mathematical standpoint, collections of behavioral constraints are unrelated to coordinated motions, because coordinated motions are subspaces of the tangent space, and constraints define subspaces of the cotangent space. However, if we are able to equip the anchor space with a metric, we can dualize the constraints (via the musical isomorphism [10]) to interpret them as defining a control distribution, including those that represent synergies.

D. Scaffolding for learning movement quickly

Humans exhibit a series of developmental milestones while learning to walk [25]. Simulation studies (see [26], and the references therein) and common practice by roboticists has shown that incorporating optimization milestones into a scaffold of nested behaviors can dramatically improve the rate at which robots can learn complex physical behaviors.

Since the pullback of a differential form is defined for any full-rank map between manifolds, our approach suggests a natural extension to a scaffold, i.e., we can just as easily have a sequence of encoding templates Q_{E_1}, \dots, Q_{E_n} (with the convention $E_0 := Q_R$) related by projections where $\phi_{n-1:n}$ maps template E_{n-1} into E_n . This gives rise to a corresponding chain of nested behavioral specifications $(\phi_{n-1:n}, \Omega_{E_n}, \gamma_{E_n})$.

A scaffold like this, where constraints are iteratively pulled back, allows a learning strategy to construct complex behaviors for highly actuated robots out of lower-DoF “*proto-behaviors*”.

Designers, be they engineers or autonomous optimization tools, could initially design a curve $x(t) \subset E_{n-1}$ that obeys a behavior specification for E_n . Then, they can use $x(t)$ to augment an existing behavior specification on E_{n-2} . In designing a new curve in E_{n-2} , we gain the ability to both *preserve* the first behavior, while enforcing a new one. As n decreases, the dimension of the corresponding encoding template grows, allowing us to constructively lift low-dimension component behaviors into increasingly complex anchors.

E. Behavior Specifications are not a planning tool

It is common in contemporary robotics to plan the motions of a complex robot (e.g. a car) using a simplified representation (e.g. a unicycle model template). Once a plan is created which meets certain feasibility heuristics, the plan is given to an optimizer which computes a detailed actuation schedule for its implementation, based on a detailed anchor model. With this in mind, a key issue in using templates for planning is having a guarantee that a planned template behavior can be realized by some choice of input to the anchor.

Much of the efficacy of our method for behavior recovery is due to not requiring this property. A key feature of our encoding templates is that we do not require that all curves in the encoding template can be realized as trajectories of the anchor; we only require that one distinguished, desired $y(t)$ can. Equivalently, we only insist that the constraints are satisfiable along the specified $y(t)$, rather than everywhere on the encoding template.

It may very well be that the combined Ω_P and Ω_D are over-determined other than on $x(t)$, and cannot be simultaneously satisfied. Thus the constraints ω_i are not suitable for planning. For example, if the template constraints corresponded to a kinematic car, the trajectories of the car other than the one distinguished car motion corresponding to our desired motion are not required to be achievable by the physical car. If the ω_i are defined over the entirety of Q_E , they could be used to classify multiple output curves as meeting or violating the constraints, but we emphasise that this is not the same as requiring every output curve to be achievable.

F. Relationship to Output Tracking

A vast literature in control theory is dedicated to the problem of “*Output Tracking*” – producing a desired trajectory of output variables. While our constraint-based optimization function offers an empirically rapid solution technique for such a problem, our contribution is more accurately reflection in the idea that the constraints ω_i *define* the output $y(t)$. We elected the constraints first, and evaluated them as output functions along a known behavior $x_0(t)$, which is how we originally obtained the definition of $y(t)$.

In our formulation, the desired output $y(t)$ is an *encoding* of the desired behavior that was generated to represent it to facilitate recovery. Part of the novelty we claim for our work is the observation that a desired behavior specification can be obtained from a known $x_0(t)$ in a very cavalier way – pretty much any set of ω , and any ϕ that meet our requirements are equally good for defining $y(t)$. Computational accuracy

constraints suggest that having the matrix ω well conditioned is advantageous, but we have found no other requirement to be of great practical importance. That $y(t)$ is a derived quantity is part of our motivation for omitting it from the notation (ϕ, ω, η) . It also motivates the adjective “encoding”, in that we have found a representation of a desired behavior, but hints that such encodings are not unique.

IV. CONCLUSION

The key contribution of our work here is a novel method for recovering robot behaviors after damage to the robot renders the previous actuation policy ineffective. We offer a key insight – although damage is complicated to understand in terms of the changes it causes to a control distribution, many common forms of damage take the form of low-rank changes to the constraints that define the robot dynamics. Thus, we propose a dual formulation for both dynamics and desired behaviors: “*behavior specifications*”, which are defined in terms of differential forms and their desired outputs. This cotangent bundle formulation has a distinct mathematical advantage in that it make it easy to encode example behaviors and recover them when low-rank changes to the constraints occur.

With this approach we have shown large speedups in the ability of physical robots to re-learn a desired behavior, and shown how a simulated system can recover to within numerical precision when the damage model is known. Our approach has ties to many existing ideas in control, theoretical mechanics, and neuromechanical control in animals. These suggest to us that the “*behavior specifications*” we propose here will help connect fields and inform our future work for many years to come.

REFERENCES

- [1] R. J. Full and D. E. Koditschek, “Templates and anchors: neuromechanical hypotheses of legged locomotion on land,” *Journal of experimental biology*, vol. 202, no. 23, pp. 3325–3332, 1999.
- [2] M. A. Sharbafi and A. Seyfarth, *Bioinspired Legged Locomotion: Models, Concepts, Control and Applications*. Butterworth-Heinemann, 2017.
- [3] A. M. Bloch, P. Krishnaprasad, J. E. Marsden, and R. M. Murray, “Non-holonomic mechanical systems with symmetry,” *Archive for Rational Mechanics and Analysis*, vol. 136, no. 1, pp. 21–99, 1996.
- [4] F. Bullo, A. D. Lewis, and K. M. Lynch, “Controllable kinematic reductions for mechanical systems: concepts, computational tools, and examples,” in *Mathematical Theory of Networks and Systems*, vol. 124, 2002.
- [5] A. M. Bloch and P. E. Crouch, “Another view of nonholonomic mechanical control systems,” in *Proceedings of 1995 34th IEEE Conference on Decision and Control*, vol. 2. IEEE, 1995, pp. 1066–1071.
- [6] A. M. Vershik and L. D. Faddeev, “Differential geometry and lagrangian mechanics with constraints,” in *Doklady Akademii Nauk*, vol. 202, no. 3. Russian Academy of Sciences, 1972, pp. 555–557.
- [7] J. L. Synge, “Geodesics in non-holonomic geometry,” *Mathematische Annalen*, vol. 99, no. 1, pp. 738–751, 1928.
- [8] A. D. Lewis, “Affine connections and distributions with applications to nonholonomic mechanics,” *Reports on Mathematical Physics*, vol. 42, no. 1-2, pp. 135–164, 1998.
- [9] V. I. Arnol’d, *Mathematical methods of classical mechanics*. Springer Science & Business Media, 2013, vol. 60.
- [10] J. M. Lee, “Smooth manifolds,” in *Introduction to Smooth Manifolds*. Springer, 2013, pp. 1–31.
- [11] J. Schmitt and P. Holmes, “Mechanical models for insect locomotion: dynamics and stability in the horizontal plane i. theory,” *Biological cybernetics*, vol. 83, no. 6, pp. 501–515, 2000.
- [12] R. Blickhan, “The spring-mass model for running and hopping,” *J. Biomechanics*, vol. 22, no. 11-12, pp. 1217–1227, 1989.
- [13] J. Ostrowski and J. Burdick, “The geometric mechanics of undulatory robotic locomotion,” *The international journal of robotics research*, vol. 17, no. 7, pp. 683–701, 1998.
- [14] A. Bloch, J. Baillieul, P. Crouch, J. E. Marsden, D. Zenkov, P. S. Krishnaprasad, and R. M. Murray, *Nonholonomic mechanics and control*. Springer, 2003, vol. 24.
- [15] W. S. Koon and J. E. Marsden, “The geometric structure of nonholonomic mechanics,” in *Proceedings of the 36th IEEE Conference on Decision and Control*, vol. 5. IEEE, 1997, pp. 4856–4861.
- [16] R. L. Hatton and H. Choset, “An introduction to geometric mechanics and differential geometry,” 2011.
- [17] G. Council, “Data-driven methods to build robust legged robots,” Ph.D. dissertation, University of Michigan, 2020.
- [18] K. C. Galloway, G. C. Haynes, B. D. Ilhan, A. M. Johnson, R. Knopf, G. Lynch, B. Plotnick, M. White, and D. E. Koditschek, “X-rhex: A highly mobile hexapedal robot for sensorimotor tasks,” University of Pennsylvania, Tech. Rep., 2010. [Online]. Available: <http://kodlab.seas.upenn.edu/Kod/Xrhextech>
- [19] S. Revzen and J. Guckenheimer, “Estimating the phase of synchronized oscillators,” *Phys. Rev. E*, vol. 78, no. 5, p. 051907, 2008.
- [20] K. Pearson, “Liii. on lines and planes of closest fit to systems of points in space,” *The London, Edinburgh, and Dublin Philosophical Magazine and Journal of Science*, vol. 2, no. 11, pp. 559–572, 1901.
- [21] M. Golubitsky and V. Guillemin, *Stable mappings and their singularities*. Springer Science & Business Media, 2012, vol. 14.
- [22] N. J. Jarque-Bou, A. Scano, M. Atzori, and H. Müller, “Kinematic synergies of hand grasps: a comprehensive study on a large publicly available dataset,” *Journal of neuroengineering and rehabilitation*, vol. 16, no. 1, p. 63, 2019.
- [23] A. Daffertshofer, C. J. Lamoth, O. G. Meijer, and P. J. Beek, “Pca in studying coordination and variability: a tutorial,” *Clinical biomechanics*, vol. 19, no. 4, pp. 415–428, 2004.
- [24] N. Jarque-Bou, V. Gracia-Ibáñez, J.-L. Sancho-Bru, M. Vergara, A. Pérez-González, and F. Andrés, “Using kinematic reduction for studying grasping postures. an application to power and precision grasp of cylinders,” *Applied ergonomics*, vol. 56, pp. 52–61, 2016.
- [25] K. E. Adolph and S. R. Robinson, “The road to walking: What learning to walk tells us about development,” *Oxford handbook of developmental psychology*, vol. 1, pp. 403–443, 2013.
- [26] J. C. Bongard, “Morphological and environmental scaffolding synergize when evolving robot controllers: artificial life/robotics/evolvable hardware,” in *Proceedings of the 13th annual conference on Genetic and evolutionary computation*. ACM, 2011, pp. 179–186.



George Council was born in Laurel, Maryland in 1988. He received his B.S. of Electrical Engineering from Montana State University, Bozeman, MT in 2012, and completed his Ph.D in the BIRDS Lab at the University of Michigan, Ann Arbor, MI in 2020.

He is currently engaged as a Post Doctoral Research Associate in the Robomechanics Lab at Carnegie Mellon University, Pittsburgh, PA. His research interests include legged robotics, hybrid dynamics and control, data-driven methods in applied mathematics, and their integration as a unified perspective. Dr. Council is a member of the American Physical Society (APS) as well as Society for Industrial and Applied Mathematics (SIAM).



Shai Revzen (M2015) holds a Ph.D. in integrative biology (U. California at Berkeley; 2009), M.Sc. in computer science (Hebrew University, Jerusalem, Israel; 2002), B.Sc. *summa cum laude* in computer science, mathematics (extended), and minor in physics (Hebrew University, Jerusalem, Israel; 1993). He is currently an Associate Professor in the departments of Electrical Engineering and Computer Science and Ecology and Evolutionary Biology (U. Michigan, Ann Arbor, USA). At UMich, he heads the Biologically Inspired Robotics and Dynamical Systems (BIRDS) Lab (<http://birds.eecs.umich.edu>). He is also a Founding Partner of Bio-Signal Analysis Ltd (Tel-Aviv, Israel), through which he holds several electrocardiology related patents, and General Manager of Izun, Inc (Ann Arbor, MI, USA). He was formerly Chief Architect R&D in Harmonic Lightwaves Inc and Harmonic Data Systems Ltd focusing on MPEG processing and satellite communications. He has published multiple journal papers and book chapters on topics of robotics, physics, biology, and applied mathematics, primarily relating to multi-legged locomotion, rapid fabrication of robots, and data-driven modeling of natural and artificial locomotion systems. Associate professor Revzen is also a member of the Society for Integrative and Comparative Biology (SICB), the American Mathematical Society (AMS), the Society for Industrial and Applied Mathematics (SIAM), and the American Physical Society (APS).